



ELSEVIER

Journal of Chromatography A, 869 (2000) 211–230

JOURNAL OF
CHROMATOGRAPHY A

www.elsevier.com/locate/chroma

Control of column temperature in reversed-phase liquid chromatography

R.G. Wolcott^a, J.W. Dolan^b, L.R. Snyder^{b,*}, Stephen R. Bakalyar^c, Megan A. Arnold^c,
Jon A. Nichols^c

^aDepartment of Chemistry, Linfield College, McMinnville, OR 97128, USA

^bLC Resources Inc., 2930 Camino Diablo, Suite 110, Walnut Creek, CA 94596, USA

^cRheodyne, L.P., Rohnert Park, CA 94927-1909, USA

Abstract

When separations by reversed-phase liquid chromatography (RP-LC) are carried out at temperatures other than ambient, resulting retention times and bandwidths can depend on the equipment used. As a result, an RP-LC separation that is adequate when carried out on one LC system may prove inadequate when the separation is repeated on a second system. In the present study, various temperature-related problems which can result in a failure of method transfer for non-ambient RP-LC methods were examined. Means for correcting for such effects and thereby ensuring method transferability are described. © 2000 Elsevier Science B.V. All rights reserved.

Keywords: Column temperature; Stationary phase, LC

1. Introduction

Recent work [1–5] has shown that the simultaneous variation of temperature T and either gradient time t_G or isocratic %B is a convenient and effective means of optimizing selectivity and maximizing sample resolution in reversed-phase liquid chromatography (RP-LC). This approach to RP-LC method development is applicable to samples of any type (acid, base or neutral; large or small molecules), can be used with low-UV detection (for acetonitrile as B-solvent, phosphate as buffer), and avoids problems in method robustness that are encountered with the use of other variables for selectivity optimization (pH, ion-pairing, tetrahydrofuran as B-solvent, etc.;

see discussion in Refs. [6–8]). Only four experimental runs are required to optimize T and t_G or %B, if commercial software (DryLab[®], version 2.0 or 3.0; LC Resources) is used to determine optimum experimental conditions [3,4,9,10].

Apart from its value for controlling selectivity, the use of elevated column temperatures in RP-LC has also been advocated for other reasons [11]. However, several studies summarized in Table 1 have drawn attention to the difficulty of accurate temperature control in liquid chromatography, especially for operation at higher temperatures. These various phenomena associated with column temperature control can in turn give rise to greatly reduced column efficiency and/or problems in method transferability. This paper describes our attempt to better understand and control column temperature, with the goal of maintaining maximum column efficiency and im-

*Corresponding author.

Table 1
Column temperature control problems in liquid chromatography

Problem	Refs.	Comment
1. Temperature of column oven (thermostat)	[7]	Oven set-point temperature may differ from actual temperature by several degrees and vary with position within the oven
2. Cycling of oven temperature	[20]	Oven temperature may vary with time
3. Equipment differences	[12,13]	Column temperature may differ from oven temperature to a degree that depends on the equipment
4. Mobile phase preheating	[7,14–16]	Mobile phase at column inlet is not at oven temperature
5. Frictional heating of mobile phase	[17–19]	Flow of mobile phase through column generates heat, especially for a large pressure drop across the column

proving method transferability during operation at higher temperatures.

2. Theory and background

Under ideal conditions, the temperature within the column will be the same at all points, constant over time, and equal to the temperature selected for the oven (unless noted otherwise, we will use ‘oven’ to describe any column heater/thermostat module). For many LC systems, the actual situation will be different. The selected temperature may not equal the oven temperature, which in turn may vary at different locations within the oven and with time. Even when the temperature is the same throughout the oven, the temperature within the column can vary both radially and axially, due to differences in temperature of the incoming solvent vs. that of the oven. The spatial and temporal temperature regime within the column is thus a complex function of the instrumental setup and conditions (column dimensions, flow-rate, mobile phase composition) and can therefore differ from one LC system to another. In this paper we define the term ‘average column temperature’ in terms of sample retention; if retention times are the same for otherwise identical separations carried out in two different HPLC systems, the average column temperature is then considered to be the same [12–19].

When the average column temperature differs

from the selected oven temperature (for whatever reasons), significant changes in sample retention (values of both k and α) can result. When a radial temperature gradient exists within the column, marked increases in bandwidth (accompanied by band distortion) are possible. It is widely appreciated that these effects can result in poor performance and questionable transferability of LC methods, especially those carried out at temperatures $>40^{\circ}\text{C}$. Our further discussion of column temperature effects will follow the outline of Table 1.

2.1. Column oven temperature (#1–3 of Table 1)

Differences in set-point vs. actual oven temperatures for commercial LC systems have been reported [7]. Oven temperature can also vary with time [20], but this is generally a less significant problem. When operating at temperatures other than ambient, it is advisable to measure the oven temperature and to confirm that it is constant with time, as was done in the present study. Finally, the temperature of the column may differ from the nominal temperature of the oven, due either to temperature gradients within the oven or slow thermal equilibration of the column under working (i.e. flow) conditions. LC ovens differ with respect to (a) thermostating mode (circulating air, block heaters, water bath, etc.), and (b) the presence or effectiveness of preheating of the mobile phase immediately prior to the column (i.e. after the sample injection valve).

2.2. Mobile phase preheating (#4 of Table 1)

If the mobile phase entering the column is at column temperature, and if frictional heating effects are negligible, solvent velocity and the rate of band migration through the column should be similar at the column center and wall. This will result in normal band broadening as illustrated in Fig. 1a (thermally equilibrated column). As a result of constant temperature conditions throughout the column (indicated by temperature values within the column, 70°C in Fig. 1), the dependence of reduced plate height h on reduced mobile phase velocity ν should be independent of temperature [21,22], and plots of h vs. ν for different temperatures should overlap. This generalization can prove useful in analyzing the effects of thermal non-ideality on band width.

The relationship of h and ν can be expressed by the Knox equation:

$$h = A/\nu + B\nu^{1/3} + C\nu \quad (1)$$

where the reduced plate height h is given by

$$h = H/d_p \quad (1a)$$

and the reduced velocity ν is

$$\nu = ud_p/D_m \quad (1b)$$

Definitions of the conventional symbols d_p , u and D_m are given in the Definition list.

Fig. 1b illustrates the situation where the incoming mobile phase temperature is lower than that of the column. When the incoming solvent is colder, there will be a radial temperature gradient because the temperature at the column wall exceeds that at the

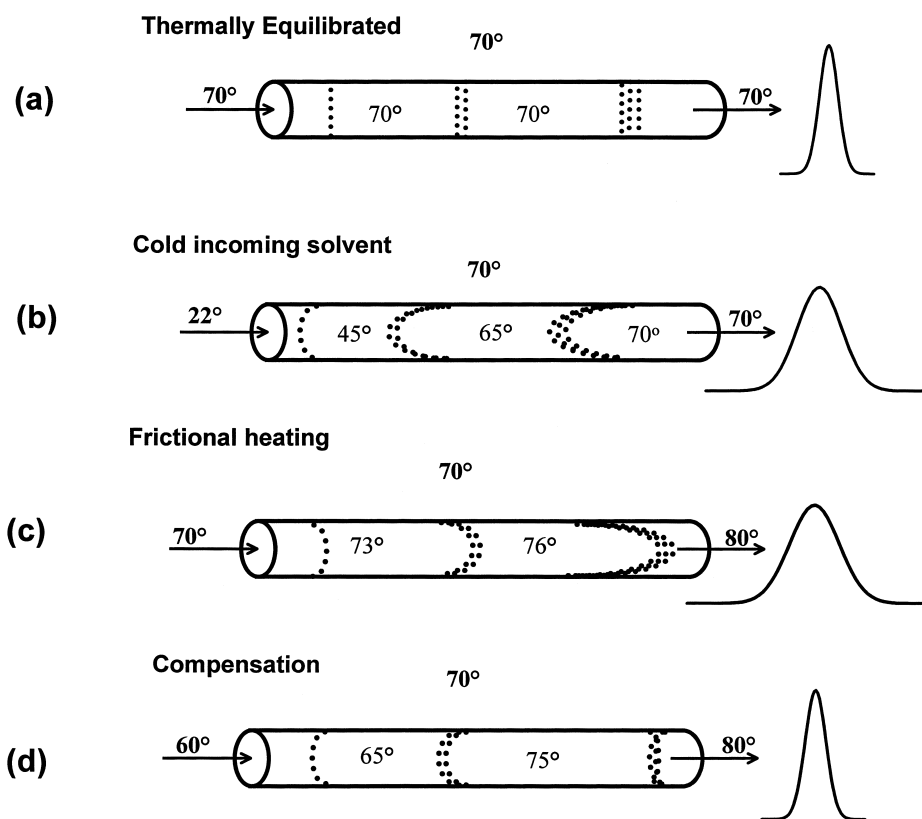


Fig. 1. Band broadening due to thermal effects. (a) Ideal case, no thermal effects; (b) effect of incoming mobile phase that is at a lower temperature than the column; (c) effect of frictional heating; (d) combined effects of cold incoming mobile phase and frictional heating. An oven temperature of 70°C is assumed. Numbers shown inside column suggest plausible solvent temperatures at column center.

column center. As the solvent moves through the column, the temperature at the column center gradually approaches that of the wall. Likewise, the solvent viscosity decreases from the column center to the wall, and band migration will tend to be faster at the wall vs. the center (especially near the column inlet). At any radial position within the column, band broadening occurs as in Fig. 1a. Additionally, due to the radial temperature gradient near the column inlet, there will be a ‘cone-ing’ of the band as shown in Fig. 1b. This can in turn result in a significant increase in band broadening and, in extreme cases, a gross distortion of the band. Should the incoming solvent temperature be greater than that of the oven, similar band broadening effects will result as in Fig. 1b, except that the band will move faster at the center of the column than near the wall.

2.3. Frictional heating (#5 of Table 1)

Flow of solvent through the column requires a pressure drop ΔP across the column length. As a result, work is done by the flowing solvent, equal to $\Delta P V_m$ for each column-volume of mobile phase flow through the column. This work is converted to heat, which causes an increase in column temperature from inlet to outlet. The consequences for band broadening are illustrated in Fig. 1c. Now the temperature is greater at the column center than near the wall, so that band migration is faster at the column center. The result is a cone-ing of the band in a direction opposite to that in Fig. 1b, but bandwidth increases in both cases. The effect of frictional heating on band broadening and distortion depends markedly on the type of oven; specifically, bandwidth may be less affected by air-bath ovens than by contact heaters or water baths when stainless steel columns are used [18].

If the incoming solvent is not at column temperature (not preheated), and if frictional heating of the solvent is significant, these two effects will tend to cancel in terms of band broadening. This is illustrated in Fig. 1d, where the band initially cones toward the inlet (cold solvent effect), but then frictional heating gradually moves the center of the band in the opposite direction. A net cancellation of these effects is possible, as in Fig. 1d; it has been shown possible to minimize increases in bandwidth

due to frictional heating by deliberate cooling of the incoming solvent [17]. Frictional heating effects are proportional to ΔP and therefore increase for longer columns, higher flow-rates, smaller particle sizes and more viscous (e.g. colder) solvent.

2.3.1. Sample retention vs. temperature

If temperature is the only parameter that is varied, solute retention k (isocratic) can be described by:

$$\log k = A - B/T_K \quad (2)$$

where A and B are constants for a given solute and T_K is the column temperature in K. We define ‘average column temperature’ such that $\log k$ is determined by this value of T_K .

3. Experimental

3.1. Equipment

A schematic showing the locations of temperature sensors in the column oven is shown in Fig. 2.

3.1.1. HPLC system

Two separate HPLC systems were used. ‘System A’ (used unless noted otherwise) consisted of a SIL-10A controller, LC-10AD VP pump, SIL-10Ai autosampler and SPD-10A VP detector set to 215 nm

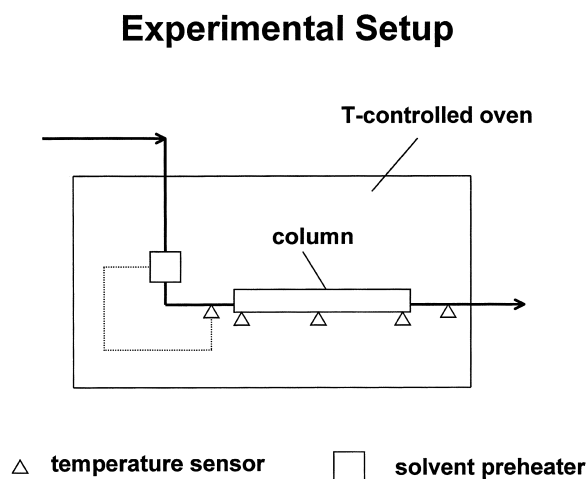


Fig. 2. Schematic of oven used in the present study.

(Shimadzu Corp., Columbia, MD). System A was equipped with either a ‘Mistral’ forced air oven (Spark Holland, Emmen, The Netherlands) or a model CH-150 block heater oven (Eldex Laboratories, Inc., Napa, CA). In the latter case the column was attached to the heated base by a 7×3 cm aluminum clamp supplied by the oven manufacturer. ‘System B’ (used to test method transferability) consisted of Shimadzu equipment similar to that of system A: SCL-10A controller, LC-10AD pump, SIL-10Ai autosampler, and SPD-10A detector set to 215 nm. The column oven for System B was a CTO-10-AS VP programmable unit (Shimadzu) with Peltier block-heating of the solvent entering the column (but no metal-to-metal contact with the column).

3.1.2. Pre-heat tubing

Various lengths of stainless steel tubing were used in system A as passive preheaters for incoming solvent. These tubes had nominal outer diameters (O.D.) of either 1/16" (0.16 cm; ‘conventional’) or 0.020" (0.008 cm; ‘thin-wall’), and internal diameters (I.D.) ranging from 0.005" (0.002 cm) to 0.012" (0.0047 cm). They were shaped to facilitate heat transfer: loose coils for good air circulation in the circulating-air oven; or flat loops for maximum contact with the heated base of the block-heater oven. When used in the latter configuration, tubes were sandwiched between two pads of four layers of aluminum foil and clamped to the heated surface over most of their length. Thermal insulating material between the clamp and upper foil layer minimized heat loss from the tube to the overlying clamp. In experiments designed to study the ability of tubing to gain heat, the column was omitted, water was used as mobile phase, and flow-rates were varied between 1 and 4 ml/min. In system B, a passive preheat tube is incorporated into the heated oven block. The exact dimensions of this tube could not be measured, but it is at least 25 cm long and the equipment manual reports its volume as 10 μ l.

3.1.3. Temperature measurements

Temperatures were monitored using a Thermes system and software (Physitemp Instruments Inc., Clifton, NJ). All thermocouples were type T copper-constantan. Temperatures of flowing solvent just

before and after the column were measured using needle probes mounted in thermally insulated PEEK tees. Oven and column temperatures were measured using electrically isolated thermocouples in the oven air or firmly clamped on the column wall near its inlet, midpoint and outlet. Column-mounted thermocouples were overlaid with thermal insulation to more accurately report the column wall temperature. The positions of the various temperature probes are shown in Fig. 2.

3.1.4. Temperature control

In experiments where incoming solvent was actively preheated, a custom, electrically-heated coil (Rheodyne, Rohnert Park, CA) of 10 μ l volume was used. Temperature of solvent emerging from the preheater module was regulated and measured by a CAL 3300 temperature controller (CAL Controls Inc., Libertyville, IL) using a type T needle thermocouple in the flowing stream as the sensing probe. The needle was in a PEEK tee which was wrapped in thermal insulation to minimize heating or cooling from the oven air.

3.2. Materials and procedures

3.2.1. Sample

The sample was a mixture of uracil (A), nitroethane (B), phthalic acid (C), 3,5-dimethylaniline (D), 4-chloroaniline (E), 3-cyanobenzoic acid (F), and 1-nitrobutane (G) in 90:10 (v/v) water/acetonitrile. The sample was chosen to (a) comprise a mixture of neutrals plus partially ionized acids and bases under the conditions of separation, and (b) provide marked changes in selectivity as a function of temperature. See the example of Fig. 3.

3.2.2. Procedures

Separations were carried out at different temperatures and flow-rates on a Zorbax 150×4.6 mm SB-C₁₈, 5 μ m d_p column (Mac-Mod Analytical, Chadd’s Ford, PA). Mobile phase was 90:10 (v/v) 50 mM potassium phosphate, pH 2.6/acetonitrile.

3.2.3. Calculations

Plate numbers N were calculated from widths at half-height, $W_{0.5}$, reported by the data system: $N =$

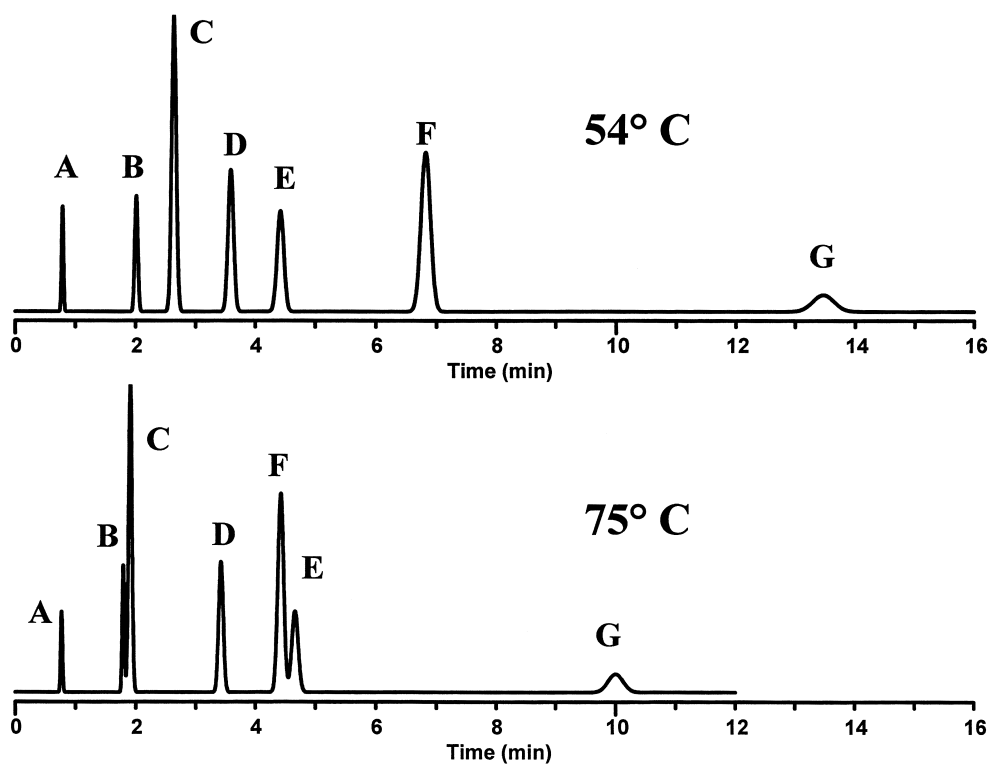


Fig. 3. Separation of present sample at 54 and 75°C. Incoming solvent preheated to oven temperature; system A, circulating-air oven. Flow rate is 2.0 ml/min; other conditions as in Experimental section.

$5.54(t_R/W_{0.5})^2$. Reduced velocities were calculated as ud_p/D_m , with $u = L/t_0$ and D_m given by the Wilke–Chang equation [23].

3.2.4. Computer simulations

Computer simulations were used in the present study to conveniently correct for differences in average column temperature between different LC equipments. The software used was Drylab[®] for Windows, Version 2.0 (LC Resources).

4. Results and discussion

4.1. Separations under ideal conditions of thermal equilibration

The present study began with a comparison of separations carried out under conditions of thermal equilibration within the column, i.e. with preheating

of the mobile phase to oven temperature prior to the column inlet. Flow rate was varied from 0.2 to 5 ml/min, at temperatures of 23, 34 and 54°C. Resulting plots of $\log h$ vs. $\log \nu$ are shown in Fig. 4 for 1-nitrobutane. Similar plots were obtained for the other six solutes, except that values of h tend to be somewhat higher for early-eluting solutes ($k < 3$), possibly as a result of extra-column effects (see Fig. 6).

Within experimental error, the data points of Fig. 4 appear to fall on a common curve, as expected for a column that is thermally equilibrated both axially and radially. If frictional heating were to affect bandwidth for the separations of Fig. 4, bands should be broader at higher flow-rates and lower temperatures that involve more viscous mobile phase. This is not the case in Fig. 4, which suggests that frictional heating was unimportant in these experiments. This was confirmed by direct measurements of temperature at the column inlet and outlet; for oven tempera-

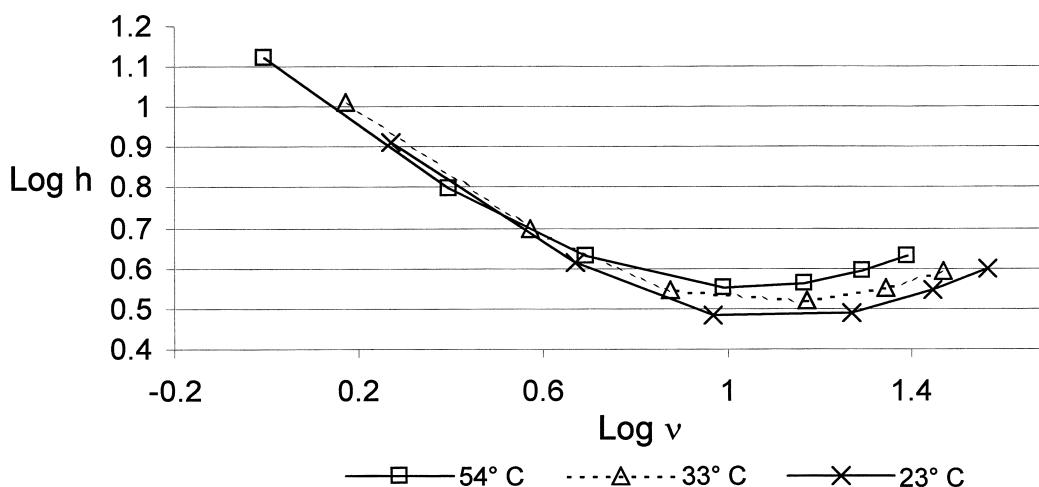


Fig. 4. Reduced parameter plot for 1-nitrobutane (G). Conditions as in Experimental section (system A, circulating-air oven).

tures of 23–75°C, temperatures at the column inlet and outlet differed by no more than 0.3°C at a flow-rate of 2.0 ml/min. Later, we will see that much larger axial temperature gradients are required for a significant effect on column plate number and h . Frictional heating was therefore considered to be insignificant in subsequent studies. However, this might not be the case for other conditions (longer columns, smaller particles, higher flow-rates, more viscous solvents) than those used in the present investigation.

4.2. Separations with incoming solvent at a temperature different from that of the oven

Due to inadequate preheating, the incoming solvent is often cooler than the oven when the oven temperature is above ambient. As a result, the average column temperature is lowered and (usually) the retention times of all bands increase. An example is shown in Fig. 5, with vertical dashed lines marking the retention times of bands C, F and G in run (a). In Fig. 5a, the separation was carried out under 'ideal' isothermal conditions (forced-air oven set to 56°C; incoming solvent actively preheated to oven temperature). In Fig. 5b, the preheat module was turned off, resulting in a drop of the incoming solvent temperature to 39.3°C at the column inlet. As a result, the average column temperature decreased (an axial gradient in temperature as in Fig. 1b is

assumed), and retention times (measured after thermal equilibration of the column for the new condition) increased, as expected. This failure to match the incoming solvent and oven temperatures in the run of Fig. 5b also results in band broadening and distortion, which is especially noticeable for bands F and G of Fig. 5b.

4.2.1. Band broadening

Fig. 6 shows reduced plate heights as a function of temperature mismatch of incoming solvent and oven (oven temperature of 54°C, 2.0 ml/min). The data for Fig. 6 were obtained using the forced air oven and active pre-heater to produce the temperature mismatches shown (x-axis). Table 2 summarizes proportional increases in reduced plate heights for a 6°C temperature mismatch and oven temperatures of 33, 54 and 74°C. Any increase in band broadening for early bands A–D is less pronounced, possibly because of larger values of h in the absence of temperature mismatch. For later bands D–G, the average increase in h for a $\pm 6^\circ\text{C}$ difference between incoming solvent and column is 8%, corresponding to a 4% decrease in sample resolution. We conclude that a temperature mismatch between solvent and column of this magnitude is acceptable. That is, so far as band widths are concerned, the incoming solvent need only be matched within $\pm 6^\circ\text{C}$ of the oven temperature. Altered retention times are not necessarily fully corrected by this adjustment of

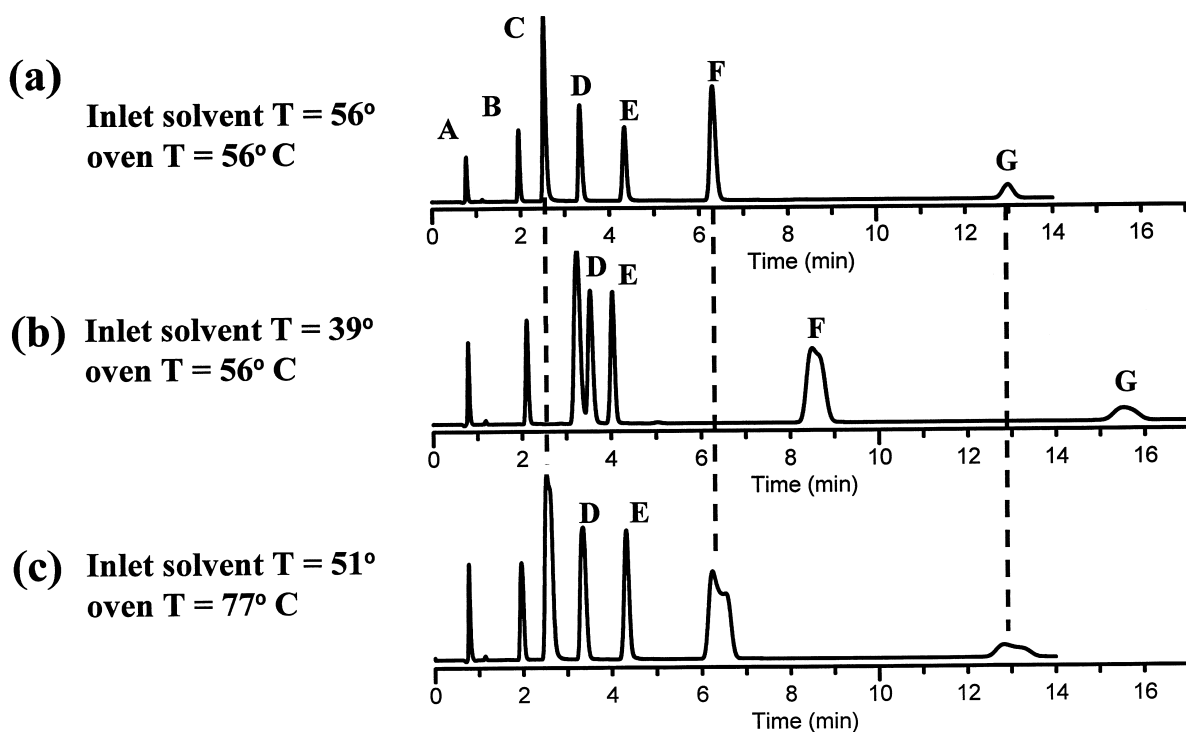


Fig. 5. Effect of the inlet solvent temperature on separation. Flow rate is 2.0 ml/min, incoming and oven temperatures shown in figure; other conditions as in Experimental section (system A, circulating-air oven).

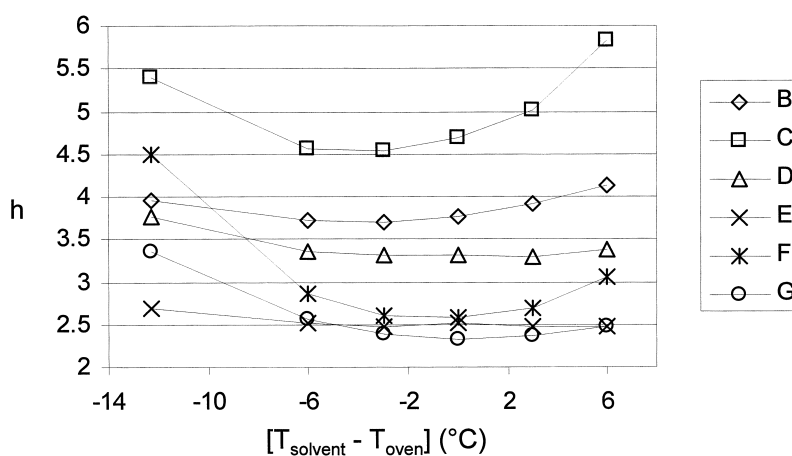


Fig. 6. Effect of difference in temperatures of inlet solvent and oven on reduced plate height h . Flow rate is 2.0 ml/min, oven temperature is 54°C, 150×4.6-mm Zorbax SB-C₁₈ column packed with 5- μ m particles; other conditions as in Experimental section (system A, circulating-air oven).

Table 2
Effect on column efficiency of mismatch of temperatures between incoming solvent and oven^a

Solute	% increase in h at given offset from indicated oven temperature ^b			
	33°C (+6°C)	54°C (−6°C)	74°C (−6°C)	Average % increase
A	2	1	−3	0
B	7	−2	−5	0
C	−	−3	−4	−4
D	−	2	3	3
E	15	0	8	8
F	20	11	−5	9
G	6	10	5	7
Average for bands E–G ^c	14	7	3	8

^a Flow rate is 2.0 ml/min, 150×4.6 mm, 5- μ m Zorbax SB-C₁₈ column; other conditions as in Experimental section.

^b Calculated as $[100*(h - h_0)/h_0]$, where h = reduced plate height with incoming solvent at the given offset from column temperature, and h_0 = reduced plate height when incoming solvent is at column temperature. Magnitude and direction of temperature offsets are in parentheses.

^c Data most accurate for later bands.

incoming solvent temperature, because the average column temperature can still differ for reasons #1–3, 5 of Table 1.

4.2.2. Changes in retention and selectivity

Values of k and α are temperature dependent, as illustrated by the example of Fig. 3. An average column temperature different from the intended value may result from temperature gradients within the oven, oven calibration error, or a mismatch of the temperatures of incoming solvent and column. The obvious remedy in these cases is to adjust oven temperature so that the average column temperature becomes equal to the intended value. For the case of solvent/column mismatch that generates axial and radial temperature gradients, can such an adjustment replicate retention obtained under exact isothermal conditions? If so, then as long as band widths are not excessively broadened by solvent/column mismatch, it should be possible to compensate for small differences in the temperatures of incoming solvent and column by simply adjusting the oven temperature. This in turn would allow a simpler adjustment of temperature conditions when an LC method is to be transferred from one system to another. That is, it would not be necessary to exactly match the temperatures of the two ovens, nor would it be necessary that the temperature of incoming solvent be exactly the same, in order to replicate separations on two different LC systems (keeping in mind that band-

widths are relatively insensitive to column temperature gradients <6°C).

The question of whether retention can be replicated with a different solvent/column temperature mismatch but equal ‘average’ column temperature is examined in Fig. 5. In the separation of Fig. 5a, there is no solvent/column mismatch. When cold solvent enters the column as in Fig. 5b, retention changes as a result of the decrease in average column temperature. In the separation of Fig. 5c, the average column temperature has been adjusted by raising the oven temperature from 56 to 77°C (with the preheater still off) to give the same retention time for the last band. As a consequence, the inlet solvent temperature changed to about 51°C. It is evident that retention times for all components in Fig. 5a and c are now essentially the same, despite this large axial temperature gradient (77–51 = 26°C). Presumably, for smaller differences in the temperatures of incoming solvent and column (e.g. <6°), an adjustment of the oven temperature can be used to create exactly the same retention (and selectivity) for two LC systems where solvent/column temperature mismatch is not identical (as it need not be, so long as bandwidths and resolution are the same within $\pm 4\%$).

We conclude that temperature discrepancies as in Table 1 can create undesirable changes in both band widths and retention times. Other conditions equal, band width can be minimized by preheating the incoming solvent to within $\pm 6^\circ\text{C}$ of the column temperature. Changes in retention and selectivity can

be eliminated by adjustments in oven temperature that achieve the same ‘average’ column temperature.

4.2.3. Temperature mismatch effects for different flow-rates and columns of different internal diameter, length or particle size

The preceding experiments were carried out with a 150×4.6-mm column packed with 5- μ m particles, at a flow-rate of 2 ml/min. A brief examination was made of the effects of change in (a) flow-rate, (b) column length or (c) internal diameter, and (d) particle size on changes in band width due to cold incoming solvent (Table 3). Increased band broadening due to inlet temperature mismatch is seen to be greater for longer columns (#3 vs. 2, #5 vs. 4), higher flow-rates (#1 vs. 3), smaller particles (#5 vs. 2) and wider columns (#6 vs. 7, where linear solvent velocity is maintained constant by varying flow-rate). There may also be an effect of the column design; e.g. #6 (Waters) vs. #2 (H-P). These trends for flow-rate, particle size and column ID can be reconciled with a simple picture of what is happening within the column. Thus, higher flow-rates should allow less time for thermal equilibration of the incoming solvent, smaller particles provide narrower bands which will be relatively more affected by band coning, and narrower columns should allow faster thermal equilibration of the solvent. A simple reason for the trends in Table 3 with column length is less obvious.

4.3. Controlling the temperature of incoming solvent

The use of LC systems which automatically adjust the temperature of the incoming solvent to match that of the column [24] is becoming more common. However, LC systems without this provision are still in widespread use, especially where autosamplers are required. For the latter case, a simple expedient is to add a length of narrow I.D. tubing just before the column (within the oven) in order to heat the incoming solvent to the column temperature. This raises two questions: (a) what tubing dimensions and type are sufficient for different experimental conditions (flow-rate, column dimensions, oven temperature, etc.), and (b) what impact will the addition of such tubing have on extra-column band broadening? We examined these two questions in order to arrive at preliminary recommendations which can help minimize problems due to cold incoming solvent.

4.3.1. Solvent heating as a function of flow-rate and pre-heat tube dimensions

Let the temperature of the incoming solvent prior to the pre-heat tube be T_1 , the temperature of the solvent leaving the pre-heat tube T_2 , and the oven temperature T_3 . Define the *fractional heating* x in the pre-heat tube as $(T_2 - T_1)/(T_3 - T_1)$. The value of x can be accurately predicted by the intuitive relationship

Table 3

Effect of column parameters on changes in reduced plate height caused by mismatch between temperatures of incoming solvent and column (all dimensions in mm; flow-rate in ml/min)

Column type	Length	Diameter	d_p	Flow	$h(-5)^a$	$h(-10)^a$
#1 SB-C ₁₈	250	4.6	0.005	3.3	18	63
#2 SB-C ₁₈	150	4.6	0.005	2	4	18
#3 SB-C ₁₈	250	4.6	0.005	2	15	45
#4 SB-C ₁₈	75	4.6	0.0035	2	-6	2
#5 SB-C ₁₈	150	4.6	0.0035	2	11	41
#6 Symmetry C ₁₈	150	4.6	0.005	2	-1	13
#7 Symmetry C ₁₈	150	2.1	0.005	0.417 ^b	-2	-3

^a Averages of % change in h for compounds E–G, computed as $100 \times (h - h_0)/h_0$. Offset of incoming solvent temperature from column temperature is in parentheses.

^b This flow-rate gives the same mobile-phase linear velocity in the 2.1-mm I.D. column as for the corresponding 4.6-mm I.D. column (#6).

$$\log(1-x) = -B(L/F) \quad (3)$$

where B (in min/cm^2) is a constant (see Appendix A for a further analysis of solvent heating and Eq. (3)). Typically, $B \approx 0.025$ for a circulating-air oven and 1/16" O.D. stainless steel pre-heat tubing with internal diameters (I.D.) of 0.005–0.012". This is illustrated in Fig. 7 for flow-rates of 1–4 ml/min, oven temperatures of 33–75°C, and tube lengths of 50–150 cm. Table 4 summarizes all plotted data of Fig. 7, which are fitted to Eq. (3) in each case. Data points for all tubes examined fall on the same line at each temperature, suggesting that over this range of tube dimensions there is no dependence of solvent heating on tube I.D. Additionally, the heating efficiency measured by the value of B is seen in Table 4 to be essentially independent of the oven temperature over the interval $T_3 - T_1$. That B is not a function of $(T_3 - T_1)$ may seem surprising at first. However, the quantity x (which is used to define B ; Eq. (3)) is *relative* to the temperature range $T_3 - T_1$. For example, assume $x = 0.9$ and $T_1 = 25^\circ\text{C}$; then $T_2 = 34^\circ\text{C}$ when $T_3 = 35^\circ\text{C}$, but $T_2 = 70^\circ\text{C}$ when $T_3 = 75^\circ\text{C}$.

4.3.2. Solvent heating as a function of other variables

Table 5 summarizes some preliminary information on the performance of pre-heat tubes of different construction or when used in a block heater instead of an air oven. We expected the heat transfer efficiency of 1/16" O.D. PEEK tubing (I.D. 0.007"; 0.0028 cm) to be lower than that of 1/16" O.D. stainless, because polymer is a poorer heat conductor than steel. Indeed, the B value was found to be only 70% of that of 1/16" O.D. stainless. Thin-wall (0.020" O.D.) stainless steel tubing was initially expected to be more efficient than 1/16" O.D. steel for temperature equilibration, i.e. a larger value of B was expected. Instead, we found the value of B for thin-wall tubing to be only 0.7 as great as that for 1/16" O.D. steel tubing, nearly identical to that found for the PEEK tubing.

We rationalize the lower value of B for thin-wall tubing in terms of (a) the high thermal conductivity of steel compared to air, and (b) the tubing surface area over which heat is collected from its surroundings. Thus, the more efficient conduction of heat

through the thin-wall tubing is counteracted by the larger diameter and greater surface area of conventional (1/16" O.D.) tubing. Our observations suggest that the surface area presented to the heated medium in a circulating-air oven primarily determines the rate of heat transfer; see also the related discussion of Ref. [25] for capillary electrophoresis.

Limited experiments with the block heater yielded values of B that appear to vary with flow-rate. For 0.010" I.D., 1/16" O.D. stainless tubing with lengths of 10–50 cm, values of B were obtained as follows: for $F = 1$, $B = 0.05 \pm 0.025$; for $F = 2$, $B = 0.08 \pm 0.04$; for $F = 3$, $B = 0.10 \pm 0.04$; for $F = 4$, $B = 0.12 \pm 0.04$. The relatively poor precision of values of B probably reflects variation in the thermal contact between heated block and tube. A further factor was the need for unheated plumbing connections. In any case, these values of B are larger than the values of Table 4 for a circulating-air oven by 2- to 5-fold. This is understandable in terms of the more efficient conduction of heat from oven to solvent by metal-to-metal contact in the block heater (vs. air-to-metal contact in an air oven). The efficiency of heat transfer should be strongly affected by how well the pre-heat coil contacts the heated metal block; see also the discussion of Ref. [13].

4.3.3. Extra-column band broadening caused by the solvent pre-heat tube

A good discussion of extra-column band broadening as a result of LC connecting tubing is provided by Ref. [26]. The extra-column band broadening W_{ec} is proportional to tube length L_t and the fourth power of tube internal diameter. For $N = 10\,000$ and a column dead-volume $V_m = 1.5$ ml (e.g. for a 150×4.6 -mm column), a 3-cm length of 0.020"-I.D. tubing should not significantly increase band widths [27]. For smaller-I.D. tubing, extra-column band broadening is much less significant; L_t can be increased as the inverse ratio of tube I.D. to the fourth power. For example, tube lengths of 7.5 m (0.005" I.D.) and 50 cm (0.010" I.D.) should be acceptable in terms of extra-column effects. Experiments were carried out with and without the addition of a 50-cm length 0.010" I.D. tubing, to see if a measurable increase in band width could be observed (2.0 ml/min, other conditions as in Fig. 3. Within experimental error,

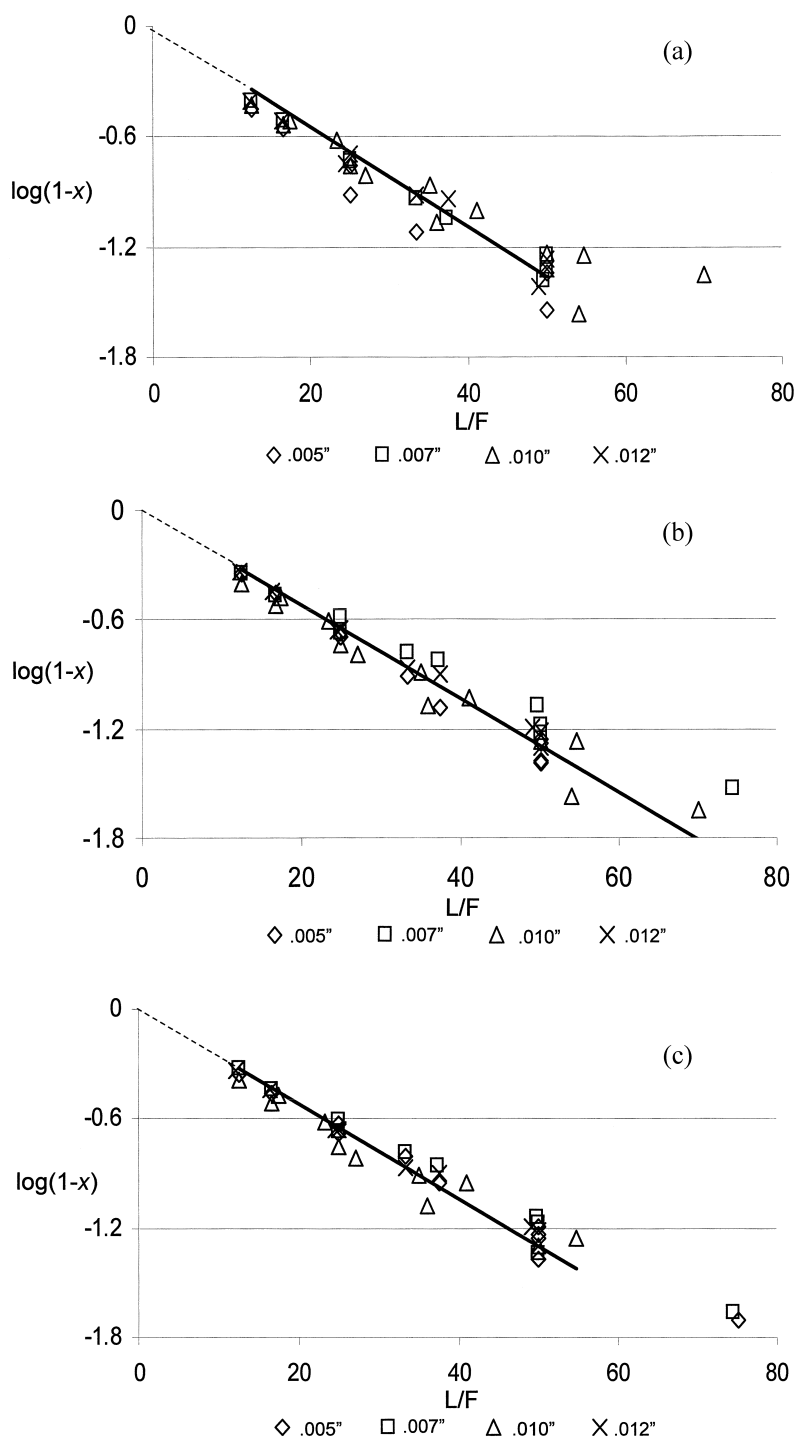


Fig. 7. Verification of Eq. (3) for thermal equilibration in a pre-heat tube. Conditions: system A, circulating-air oven, 1/16" O.D. stainless steel tubing with internal diameters as shown in the legend; flow-rates of 1–4 ml/min, and tube lengths of 50–150 cm. (a) Incoming solvent temperature $T_1 = 24^\circ\text{C}$, oven temperature $T_3 = 35^\circ\text{C}$; (b) $T_1 = 25^\circ\text{C}$, $T_3 = 55^\circ\text{C}$; (c) $T_1 = 24^\circ\text{C}$, $T_3 = 75^\circ\text{C}$. Units of (L/F) are min/cm^2 .

Table 4
Heat gain efficiency of 1/16" O.D. pre-heat tubes as a function of temperature differential in circulating air oven: summary of data of Fig. 7

Data source	Incoming solvent (°C)	Oven (°C)	B (min/cm ²) in Eq. (3)
Fig. 7a	24	35	0.026
Fig. 7b	25	55	0.025
Fig. 7c	24	75	0.025

Table 5
Comparison of heat gain efficiency of various preheating arrangements

Type of pre-heat tube/oven	B/B_0^a
PEEK (1/16" O.D.)/circulating air oven	0.7
Thin-wall stainless (0.020" O.D.)/circulating air oven	0.7
Stainless (1/16" O.D.)/block heater oven	2–5 ^b

^a B in Eq. (3) for indicated arrangement (e.g. PEEK tubing) divided by $B = B_0$ for 1/16" O.D. stainless steel tubing in circulating-air oven (value from Table 4).

^b B/B_0 varies with flow-rate: $B/B_0 = 2$ for $F = 1$; $B/B_0 = 5$ for $F = 4$.

the addition of this tubing length resulted in no change in band width for the present sample.

4.3.4. Recommended pre-heating tube dimensions for different conditions

Based on Eq. (3) with $B = 0.025$, it is possible to estimate minimum lengths of pre-heat tubing that will avoid significant band broadening due to cold incoming solvent (Table 6). In order to minimize extra-column band broadening, the smallest possible tube I.D. is recommended (e.g. 0.005–0.007"). It is

Table 6
Recommended lengths of 1/16" O.D. stainless steel pre-heat tubing for various temperature differentials and flow-rates in a circulating-air oven^a

$T_3 - T_1$ (°C) ^b	Recommended length of tubing (cm) ^c		
	$F = 1$ ^d	$F = 2$ ^c	$F = 4$ ^c
10	9 (2)	18 (6)	36 (26)
30	28 (4)	56 (14)	112 (56)
50	37 (3)	74 (13)	147 (52)
70	43 (3)	86 (12)	172 (50)

^a Assumes connection to a 150×4.6-mm column packed with 5- μ m particles at 2 ml/min. Values for identical tubing in a block heater are 0.2–0.5 as large. Tubing I.D. does not affect these values, but small I.D. values are preferred in order to minimize extra-column band broadening (e.g. 0.005" I.D.), while wider I.D. tubing may be required at high flow-rates in order to avoid excessive pressures.

^b Oven temperature T_3 minus ambient temperature T_1 .

^c Maximum tube pressure in atm (see text).

^d Flowrate in ml/min.

also advisable to use an in-line 0.5- μ m porosity filter to prevent blockage of narrow pre-heat tubes. Shorter pre-heat tubes can be used for lower flow-rates (<2 ml/min), and shorter (<150 mm) or smaller-I.D. (<4.6 mm) columns. Estimated *maximum* pressure drop values (atm) for the pre-heat tubing of Table 6 are given in parentheses, based on the use of 50% methanol/water as mobile phase and 0.005" I.D. tubing. For flow-rates >2 ml/min, it may be desirable to substitute 0.007"-I.D. tubing, which would reduce these pressure drop values of Table 6 by 75%. Note that the tube lengths of Table 6 are very likely affected by the design of the forced-air oven, so that these values may change when ovens other than the one used here are employed.

4.4. Minimizing problems in method transfer for non-ambient oven temperatures

The preceding discussion and quantitative relationships as regard solvent preheating apply mainly for a restricted set of experimental conditions: circulating-air oven, 10% acetonitrile/buffer, and a 150×4.6-mm column of 5- μ m particles. The use of other conditions should not seriously affect our following recommendations, however, if differences highlighted in Tables 3 and 5 are kept in mind. An actual transfer of a method between LC systems A and B (see Experimental section) will serve as illustration. In this example, we can assume adequate solvent

preheating for both systems. Our target (Fig. 8a) was a separation run on system A at an oven setpoint of 40°C. After completion of the run the column was moved to system B, where two separations were made at oven setpoints of 40 and 50°C with all other conditions identical to those for the target separation. System A was supplemented with a 50-cm long 1/16" O.D. × 0.007" I.D. preheat tube (16 µl volume) clamped in its block oven. System B used the Shimadzu oven, which has a built-in preheat tube (10 µl). Despite the use of the same nominal setpoint temperature, differences in average column temperature for systems A and B were not unexpected, because the two systems are of different construction. In system A, a significant fraction of the

column's metal exterior is clamped to the heated surface. In system B, there is no significant metal-to-metal contact between heated surface and column. Here, most of the heat transfer occurs from the warmed solvent as it passes through the column.

Fig. 8b shows that the separation at 40°C on B is not adequate (nor was the separation at 50°C, not shown). Computer simulation based on data from these two runs on B (Fig. 8c) predicted an excellent match to the target separation at a setpoint for oven B of 44.5°C. A final run on B set to 44.5°C gave the separation in the lower trace of Fig. 8d, which agrees closely with both the simulation of Fig. 8c and the original separation on system A (Fig. 8a).

The present rules for temperature control should

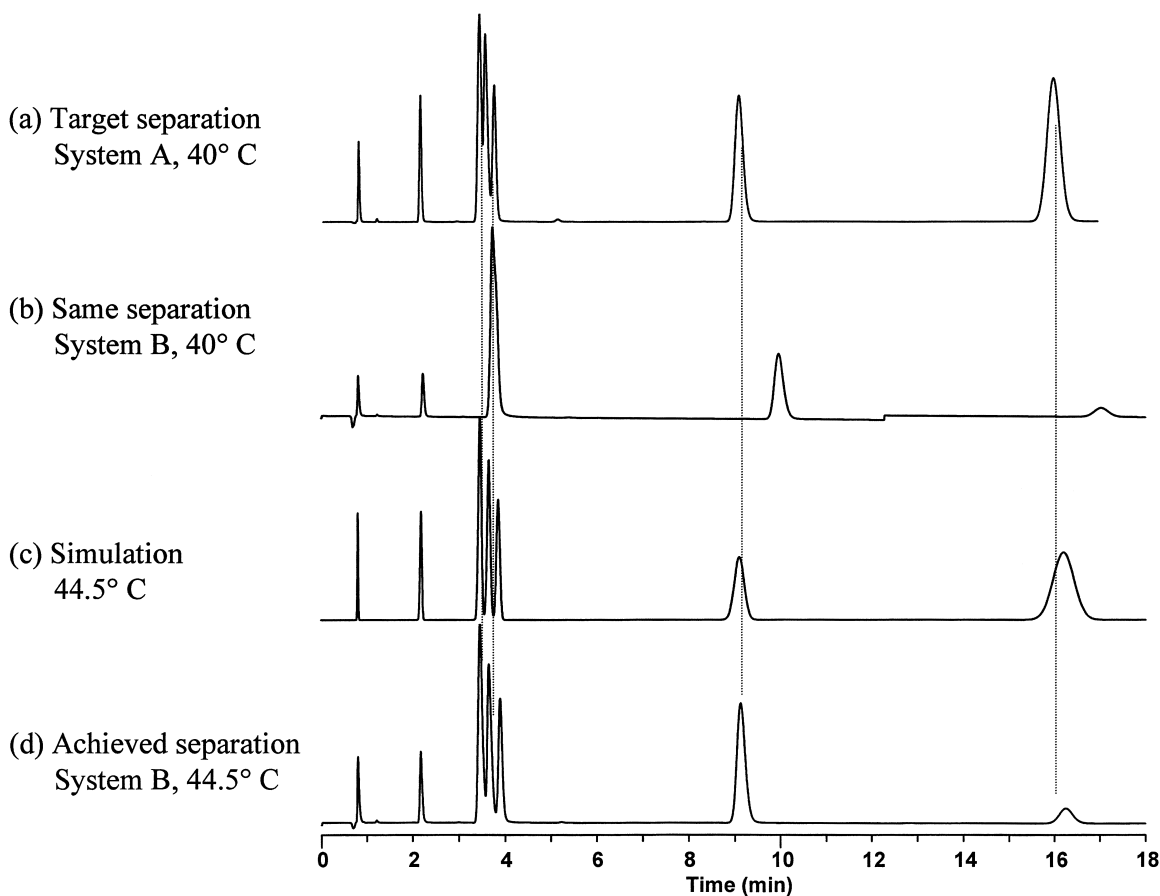


Fig. 8. Illustration of successful transfer of a separation method between LC systems using computer simulation (see text for details). All conditions nominally identical in both systems, except oven temperatures set as indicated. (Step in baseline of (b) at 12.3 min due to reset of detector zero.)

be kept in mind at the beginning of method development. If column temperature is to be varied during method development, the first step is to ensure that solvent entering the column is within $\pm 6^\circ\text{C}$ of the oven temperature for all temperatures under consideration. This can be determined by comparing column plate numbers for operation at the lowest vs. highest temperatures. If values of N are decreased by more than 10% at the higher temperature (especially if accompanied by increase peak asymmetry), additional solvent pre-heating is probably beneficial. Tables 5 and 6 provide guidelines for the addition of pre-heat tubing within the oven, if necessary. Following this step, final conditions of temperature and other variables can be determined during method development.

When a method is transferred to a second LC system (system B), the first consideration is to match solvent and column temperatures so as to avoid excess band broadening or peak distortion. If it is not known whether system B can adequately pre-heat the solvent, it is simplest to carry out the separation with the same (nominal) conditions as for the original method. If plate numbers for later-eluting sample bands are $< 80\%$ of corresponding values in the original separation, incomplete thermal equilibration of incoming solvent is the likely cause. Tables 5 and 6 provide guidance for the correction of this problem. If unacceptable differences in retention (and resolution) are observed at this point, a second run should be carried out where only temperature is changed. The two runs will establish the dependence of retention on temperature, allowing an adjustment of the oven temperature to provide the same retention with both systems. Thus, two runs can be carried out with system B, with temperatures that bracket the value of T specified by the method for system A. Eq. (2) can be assumed to be valid over a narrow range in T_K , thus allowing k for a critical band i to be calculated as a function of T . A measured temperature for system B can then be determined which will give the same value of k for band i with system B as for system A. Eq. (2) can also be used to derive

$$\log \alpha = A' + B'/T_K \quad (4)$$

which is of the same form as Eq. (2). If α for one band-pair i/j varies markedly with T , a similar

procedure can be used to select a value of T for system B that gives the same value of α for i/j with both systems. The latter procedure might be preferred when sample resolution is strongly dependent on T , and where other conditions (%B, pH, etc.) are not closely controlled between systems A and B. Computer simulation (e.g. DryLab) can also be used in a similar way to more conveniently match retention times for all bands between the two systems.

5. Conclusions

Column thermostating devices from different manufacturers vary widely in their design. As a result, LC separations carried out at temperatures much different from ambient (e.g. $T > 40^\circ\text{C}$) can be quite different when one LC system is used in place of another – as during method transfer (Fig. 8a,b provide an example). When the use of elevated column temperatures is planned during method development, it is advisable that the mobile phase entering the column be adjusted to within $\pm 6^\circ\text{C}$ of the oven temperature. This will minimize additional band broadening which can result from radial temperature gradients within the column. Unless provided for by the LC system, it is recommended that incoming solvent be routed through a suitable length of 0.005–0.012"-I.D. (0.002–0.005 cm), 1/16"-O.D. (0.16 cm) stainless steel tubing that is connected to the column inlet and placed within the oven.

The ability of a pre-heat tube of given outer diameter (O.D.) and type (e.g. SS vs. PEEK) to adjust solvent temperature appears to be similar for different tube I.D. values (0.005–0.012"). Since extra-column band broadening increases as the fourth power of tube I.D., the smallest possible tube I.D. is recommended (0.005"), consistent with the pressure drop across the tube. The heat transfer efficiency of a stainless-steel (SS) pre-heat tube is two to five times greater in a block heater (metal-to-metal contact) than in a circulating-air oven (air-to-metal contact). Recommended lengths of 1/16"-O.D. SS pre-heat tubing for different flow-rates and (circulating-air) oven temperatures are summarized in Table 6. It was found that thin-wall (0.020" O.D.) SS tubing was less effective than 1/16"-OD tubing for thermal transfer to the mobile phase, presumably due to the more

efficient heat collection by wider-diameter tubing (having a greater surface area).

When a method is transferred to another LC system, a similar provision for solvent pre-heating must be made. Operating pressures >150 atm, as when high flow-rates, small particles, or long columns are used, may lead to further band broadening as a result of frictional heating of the mobile phase. In this case, it can be advantageous to lower the temperature of the incoming solvent.

The average temperature of the column determines retention and temperature-related selectivity, regardless of temperature gradients within the column. Thus, the column does not need to be at complete thermal equilibrium for repeatable retention when using a different HPLC system (where thermal equilibration may be less [or more] complete). As long as excess band broadening due to cold incoming solvent or frictional heating is minimized (by adjusting the temperature of incoming solvent), adjustment of the oven temperature to provide the same average column temperature can ensure the same sample retention when a method is transferred from one HPLC equipment to another. This adjustment of average column temperature can be simplified by the use of appropriate computer simulation software.

6. Definition list

A, B, C	coefficients in Eqs. (1)–(3)
A–G	labels for compounds in present sample; see Experimental section
d_p	column packing particle diameter (μm)
D_m	solute diffusion coefficient (cm^2/s)
F	flow-rate (ml/min)
h	reduced plate height, equal to H/d_p
H	plate height, equal to L/N (cm)
I.D.	internal diameter
k	solute retention factor
L	column length (cm)
L_t	pre-heat tube length (cm)
LC	liquid chromatography
O.D.	outside diameter
RP-LC	reversed-phase liquid chromatography
SS	stainless steel
t_0	column dead-time (min)
T	temperature ($^{\circ}\text{C}$)

T_K	temperature in K
T_1, T_2, T_3	temperature, respectively, for ambient conditions, mobile phase leaving the pre-heat tube, and oven ($^{\circ}\text{C}$) (Eq. (3)); also, different values of T
t_R	retention time (min)
u	linear velocity of mobile phase within the column, equal to L/t_0
V_m	volume of mobile phase within the column
W_{ec}	width of a band due to extra-column effects; specifically, the width of a small injected volume after passing through the pre-heat tube (min)
$W_{0.5}$	bandwidth at half height (min)
x	fractional heating of mobile phase in the pre-heat tube, equal to $(T_2 - T_1)/(T_3 - T_1)$
α	separation factor
γ	obstruction factor for reduction of D_m by column packing
ΔP	pressure drop across the column (psi)
ν	reduced velocity, equal to ud_p/D_m

Acknowledgements

The present study was supported in part by a Small Business Innovation Research (SBIR) grant from the National Institutes of Health (US Department of Health and Human Services).

Appendix A. Heat transfer in a pre-heat tube

Symbols used in this section are defined within the section and may differ from the symbols of the Definition list.

A.1. Introduction

The heat transfer for a circular tube used as a pre-column mobile phase heater is analyzed here, using relationships from Ref. [28]; see Fig. 9. An outer flow of hot air with a temperature of T_{air} (K) flows across a tube normal to the tube axis. Mobile phase enters the tube with a mean inlet temperature of $T_{m,i}$, picks up heat as it travels through the tube,

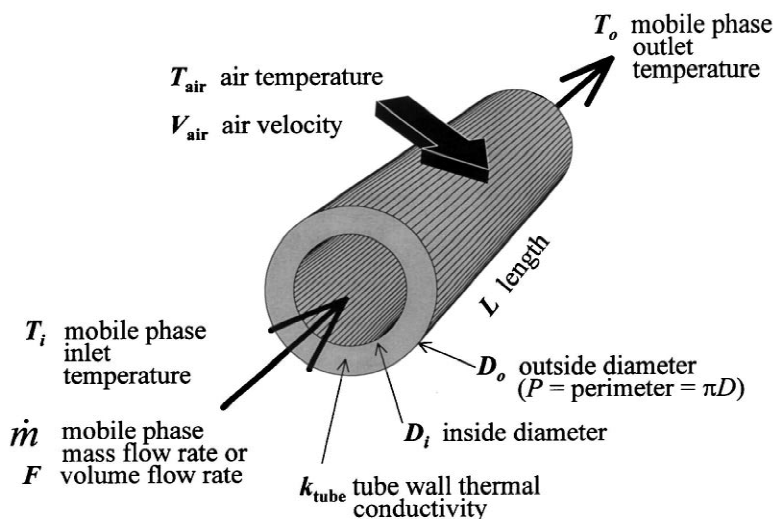


Fig. 9. Schematic representation of mobile phase heating in a pre-heat tube.

and exits with a mean outlet temperature, $T_{m,o}$. We wish to know how the outlet temperature depends on the system variables: (i) the dimensions and material of the tube, (ii) the inlet temperature, flow-rate, and physical properties of the mobile phase, and (iii) the temperature and flow-rate of the air.

A.2. Heat transfer inside a tube

The form of Newton's law of cooling that applies to flow through a tube is:

$$q'' = h(T_s - T_m) \quad (\text{A.1})$$

where q'' is the *convective heat flux* (W/m^2) or rate of heat transfer per unit area, and T_s and T_m refer to surface and mean fluid temperatures, respectively. The constant of proportionality h ($\text{W}/\text{m}^2 \cdot \text{K}$) is the *convection heat transfer coefficient*.

Applying the principal of conservation of energy for any differential (infinitesimal) control volume along the tube axis, the convective heat flux to the fluid (i.e. mobile phase) must equal the rate at which the fluid thermal energy increases, assuming no net work is done in moving the fluid through the tube. Thus the differential convective heat flux is:

$$dq'' = h m c_p dT_m \quad (\text{A.2})$$

where c_p ($\text{J}/\text{kg} \cdot \text{K}$) is the specific heat at constant pressure, and \dot{m} is the mass flow-rate (kg/s).

The mean temperature as a function of tube length is:

$$\frac{dT_m}{dx} = \frac{q''P}{m c_p} = \frac{P}{m c_p} h(T_s - T_m) \quad (\text{A.3})$$

where P is the inside perimeter of the tube. From this we can determine the mean temperature, T_m , as a function of tube length.

Further analysis is related to the convective heat transfer coefficient, h , which in turn depends on the surface thermal conditions, i.e. whether the surface is at constant surface heat flux or at constant surface temperature. We will assume a constant surface temperature of the tube wall, although these conditions do not strictly exist in the present experimental system. Some parts of the pre-heat tubing were exposed to air that had already passed over other parts of the tubing. Air temperature around the second-pass tubing was measured and found to be lower than the incoming air from the heating coils. The constant temperature case allows for a tractable analysis that should provide at least a qualitative interpretation of the experimental observations.

Define ΔT as $T_s - T_m$, the difference between the surface temperature and the mean fluid temperature. By separating variables, integrating from tube inlet to outlet, and using the definition of the average heat transfer coefficient, \bar{h} , Eq. (A.3) leads to:

$$\frac{\Delta T_o}{\Delta T_i} = \frac{T_s - T_{m,o}}{T_s - T_{m,i}} = \exp \left[-\frac{PL}{\dot{m}c_p} \bar{h} \right] \tag{A.4}$$

A.3. Heat transfer for the complete system: air to tube wall to fluid

Consider now the system at hand, in which the heat must transfer not just from the internal surface of the tube to the mobile phase, but also from external air flowing normal to the tube axis. Next, substitute for \bar{h} in Eq. (A.4) an overall average heat transfer coefficient, \bar{U} , that is the sum of the three individual heat transfer coefficients: convection from air to tube outer surface, conduction through the tube wall, and convection from tube inner surface to fluid. Also, substitute the free-stream air temperature, T_{air} , for the tube inner wall surface temperature, T_s .

$$\frac{\Delta T_o}{\Delta T_i} = \exp \left[-\frac{PL}{\dot{m}c_p} \bar{U} \right] \tag{A.5}$$

We define this quotient as the temperature fractional error x :

$$\begin{aligned} \text{fractional error } x &= \frac{\Delta T_o}{\Delta T_i} = \frac{T_{air} - T_{m,o}}{T_{air} - T_{m,i}} \\ &= \frac{\text{outlet error}}{\text{inlet error}} \end{aligned} \tag{A.6}$$

If the air temperature is the desired temperature for the fluid, then ΔT_o is the outlet fluid temperature

error, and ΔT_i is the inlet fluid temperature error. Rearranging, substituting, and using the volume flow-rate, F , instead of the mass flow-rate:

$$\ln x = -\frac{PL}{c_p \dot{m}} \bar{U} = -\left(\frac{KP\bar{U}}{c_p}\right)\left(\frac{L}{F}\right) \tag{A.7}$$

Eq. (A.7) appears to have a reasonable form, as it predicts that the fractional error will become smaller with increased length and decreased fluid flow-rate. The outlet error as a fraction of the inlet error decays exponentially with tube length, going from a quantity of 1 at the inlet to 0 at the outlet of a tube that is long enough to achieve thermal equilibrium. The longer the tube, the smaller the temperature difference between air and emerging fluid. This is illustrated in Fig. 10. Eq. (A.7) lets us plot $\ln x$ as a function of the quotient L/F . But we must know the expression for the average overall heat transfer coefficient, \bar{U} , which is the sum of three terms: $\bar{U} = [\text{air-tube convection term}] + [\text{tube wall conduction term}] + [\text{tube-fluid convection term}]$. Heat transfer theory predicts that these terms have the following form:

$$\bar{U} = \left\{ \left[\frac{D_i}{D_o \bar{h}_o} \right] + \left[\left(\frac{D_i}{2k_w} \right) \ln \frac{D_o}{D_i} \right] + \left[\frac{1}{\bar{h}_i} \right] \right\}^{-1} \tag{A.8}$$

where D_o is the outside diameter (m) of the tube, D_i is the inside diameter, \bar{h}_o is the average heat transfer

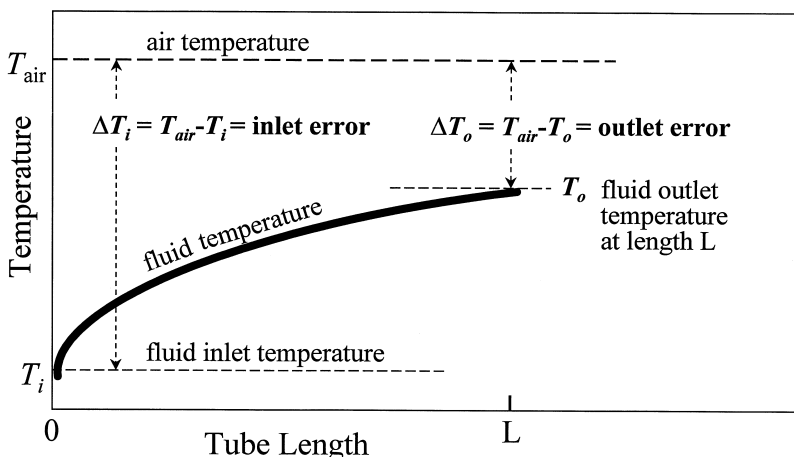


Fig. 10. Mean fluid temperature vs. length of the pre-heater tube (see Appendix A for details). The ratio $\Delta T_o/\Delta T_i$ is defined as the fractional error. It is 1 at the inlet and approaches 0 for long tubes.

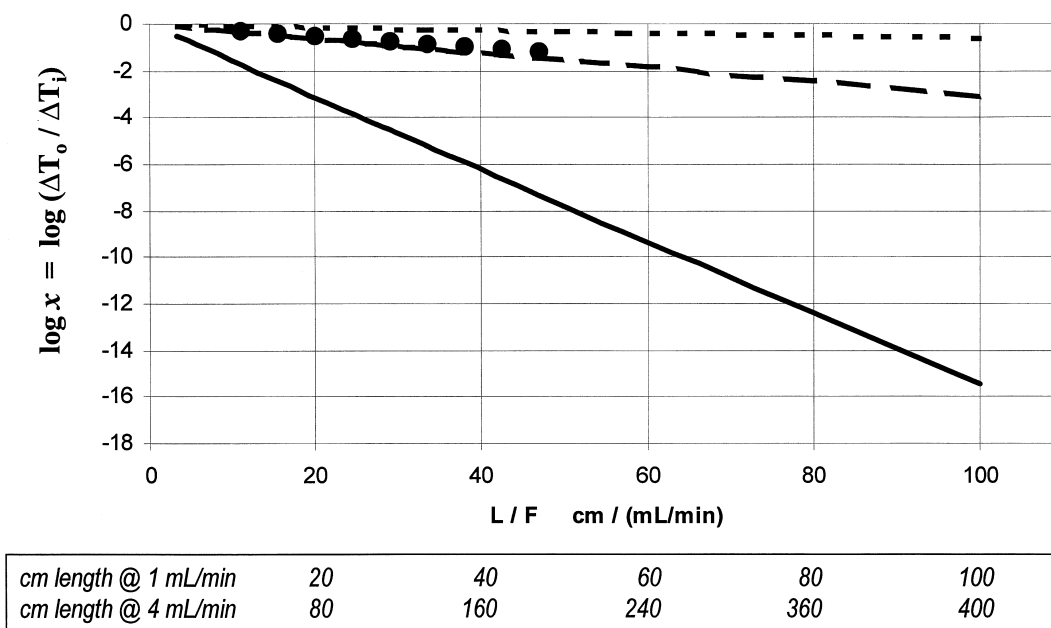


Fig. 11. Theoretical calculations vs. experimental results. The three theoretical plots are for the following conditions. All theoretical inside diameters are 0.010 inches. Solid line=1 m/s air, 0.063-inches O.D. tube; long dashed line=0.01 m/s air, 0.063-inches O.D. tube; short dashed line=1 m/s air, 0.020-inches O.D. tube. The experimental data, plotted as solid circles, was for tubing of 0.063-inches O.D. and I.D. of 0.005 and 0.012 inches (there being no measurable difference between the inside diameters).

coefficient at the air–tube boundary, and \bar{h}_i is the average heat transfer coefficient in the fluid, and k_w is the thermal conductivity of water, assumed to be the fluid in this analysis. Calculation of the tube wall term is straightforward. The other two terms require determining the heat transfer coefficients for both boundaries. \bar{h}_o is determined using equations that include the Nusselt numbers determined from empirical engineering data for this type of system. \bar{h}_i can also be found from equations. The calculations, not shown here, are based on the equation of Churchill and Bernstein ([28]; also p. 413 of Ref. [29]).

A.4. Results of theoretical calculations

Fig. 11 plots experimental data and theoretical calculations using a log form of Eq. (A.7). Comparing the two sets of curves, and assuming the theory applies, the experimental data implies an oven air velocity of ~ 0.01 m/s. The air velocity was not measured, but estimated to be at least 0.1 m/s. This

means that, as we have already suggested, the theoretical model is inadequate. At the very least, the assumption of constant surface temperature is inappropriate. However, there is agreement between theory and observation as to the general relationship between the fractional error and the tube length and mobile phase flow-rate. The form of the equation found for the experimental data (Eq. (3)) agrees with that of Eq. (A.7). Furthermore, calculations based on Eq. (A.7) (not shown here) predict a significant dependence of heating efficiency on tube O.D. This is consistent with our experimental observations.

References

- [1] P.L. Zhu, J.W. Dolan, L.R. Snyder, D.W. Hill, L. Van Heukelem, T.J. Waeghe, J. Chromatogr. A 756 (1996) 51.
- [2] P.L. Zhu, J.W. Dolan, L.R. Snyder, N.M. Djordjevic, D.W. Hill, J.-T. Lin, L.C. Sander, L. Van Heukelem, J. Chromatogr. A 756 (1996) 63.
- [3] J.W. Dolan, L.R. Snyder, N.M. Djordjevic, D.W. Hill, D.L. Saunders, L. Van Heukelem, T.J. Waeghe, J. Chromatogr. A 803 (1998) 1.

- [4] J.W. Dolan, L.R. Snyder, D.L. Saunders, L. Van Heukelem, J. Chromatogr. A 803 (1998) 33.
- [5] J.W. Dolan, L.R. Snyder, N.M. Djordjevic, D.W. Hill, T.J. Waeghe, J. Chromatogr. A 857 (1999) 1.
- [6] L.R. Snyder, *Today's Chemist at Work* 5 (1996) 29.
- [7] P.L. Zhu, L.R. Snyder, J.W. Dolan, N.M. Djordjevic, D.W. Hill, L.C. Sander, T.J. Waeghe, J. Chromatogr. A 756 (1996) 21.
- [8] L.R. Snyder, J. Chromatogr. B 689 (1997) 105.
- [9] I. Molnar, L.R. Snyder, J.W. Dolan, LC·GC Int. 11 (1998) 374.
- [10] J.W. Dolan, L.R. Snyder, LC·GC 17 (April 4S) (1999) S17.
- [11] B. Ooms, LC·GC 14 (1996) 306.
- [12] J. Paesen, J. Hoogmartens, LC·GC 10 (1992) 364.
- [13] P.-L. Zhu, J.W. Dolan, LC·GC 14 (1996) 944.
- [14] S. Abbott, P. Achener, R. Simpson, F. Klink, J. Chromatogr. 218 (1981) 123.
- [15] S.M. McCown, D. Southern, B.E. Morrison, D. Garteiz, J. Chromatogr. 352 (1986) 483.
- [16] D.M. Djordjevic, P.W.J. Fowler, F. Houdiere, J. MicroSepar. 11 (1999) 403.
- [17] N.H.C. Cooke, B.G. Archer, K. Olsen, A. Berick, Anal. Chem. 54 (1982) 2277.
- [18] H. Poppe, J.C. Kraak, J. Chromatogr. 282 (1983) 399.
- [19] A. Brandt, G. Mann, W. Arlt, J. Chromatogr. A 769 (1997) 109.
- [20] J. Paesen, J. Hoogmartens, LC·GC 8 (1990) 696.
- [21] J.H. Knox, M. Saleem, J. Chromatogr. Sci. 7 (1969) 614.
- [22] J.H. Knox, Adv. Chromatogr. 38 (1998) 1.
- [23] C.R. Wilke, P. Chang, Am. Inst. Chem. Eng. 1 (1955) 264.
- [24] H. Schrenker, Hewlett-Packard J. 3 (April) (1984) 24.
- [25] M.S. Bello, P.G. Righetti, J. Chromatogr. 606 (1992) 103.
- [26] R.P.W. Scott, P. Kucera, J. Chromatogr. Sci. 9 (1971) 641.
- [27] L.R. Snyder, J.J. Kirkland (Eds.), 2nd ed., *Introduction to Modern Liquid Chromatography*, Wiley-Interscience, New York, 1979, pp. 86–88.
- [28] F. Churchill, M. Bernstein, J. Heat Transfer 99 (1977) 300.
- [29] F.P. Incropera, D.P. De Witt, *Fundamentals of Heat and Mass Transfer*, 3rd ed., Wiley, New York, 1990.